Published in final edited form as:

Neuroscience. 2017 October 11; 361: 93–107. doi:10.1016/j.neuroscience.2017.08.014.

Whole-Transcriptome Microarray Analysis Reveals Regulation of Rab4 by RBM5 in Neurons

Travis C. Jackson[1,2], **Shawn E. Kotermanski**[3], and **Patrick M. Kochanek**[1,2]

Primary Laboratory [1]University of Pittsburgh School of Medicine, Safar Center for Resuscitation Research, Children's Hospital of Pittsburgh of UPMC, John G. Rangos Research Center – 6th Floor, 4401 Penn Avenue, Pittsburgh, PA 15224

Secondary Location [2]University of Pittsburgh School of Medicine, Department of Critical Care Medicine, Scaife Hall, 3550 Terrace Street

Secondary Location [3]University of Pittsburgh School of Medicine, Department of Pharmacology and Chemical Biology, Bridgeside Point Building 1, 100 Technology Drive

Abstract

RNA binding motif 5 (RBM5) is a nuclear protein that modulates gene transcription and mRNA splicing in cancer cells. The brain is among the highest RBM5 expressing organ in the body but its mRNA target(s) or functions in the CNS have not been elucidated. Here we knocked down (KO) RBM5 in primary rat cortical neurons and analyzed total RNA extracts by gene microarray vs. neurons transduced with lentivirus to deliver control (non-targeting) shRNA. The mRNA levels of Sec23A (involved in ER-Golgi transport) and the small GTPase Rab4a (involved in endocytosis/protein trafficking) were increased in RBM5 KO neurons relative to controls. At the protein level, only Rab4a was significantly increased in RBM5 KO extracts. Also, elevated Rab4a levels in KO neurons were associated with decreased membrane levels of oligomeric serotonin transporters (SERT). Finally, RBM5 KO was associated with increased uptake of membrane-derived monomeric SERT. Significance: Rab4a is involved in the regulation of endocytosis and protein trafficking in cells. In the CNS it regulates diverse neurobiological functions including (but not limited to) trafficking of transmembrane proteins involved in neurotransmission (e.g. SERT), maintaining dendritic spine size, promoting axonal growth, and modulates cognition. Our findings suggest that RBM5 regulates Rab4a in rat neurons.

Graphical abstract

Corresponding Author: Travis C. Jackson, Ph.D., University of Pittsburgh School of Medicine, Safar Center for Resuscitation Research, Children's Hospital of Pittsburgh of UPMC, John G. Rangos Research Center – 6th Floor, 4401 Penn Avenue, Pittsburgh, PA 15224, jacksontc@upmc.edu.

AUTHOR CONTRIBUTIONS

TCJ conceived and designed the experiments. TCJ and SEK performed experiments. TCJ and PMK contributed to data analysis and interpretation. TCJ, PMK, and SEK contributed to writing the manuscript.

CONFLICTS OF INTEREST

The authors declare no other conflicts of interest.

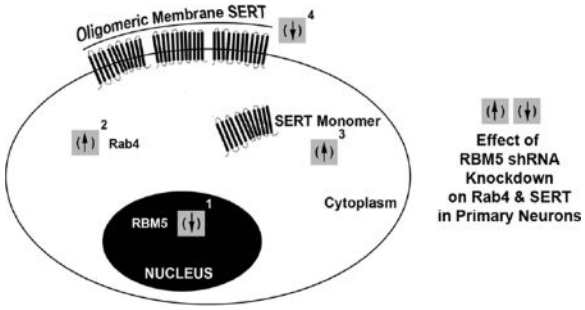

Keywords

RBM5; Rab4; Neuron; Serotonin Transporter; Endocytosis

INTRODUCTION

RNA binding proteins (RBPs) regulate cellular RNA homeostasis (Glisovic et al., 2008, Castello et al., 2016). Recent studies suggest that RBP dysregulation plays a role in the development of cancer (Wu et al., 2015), cardiovascular (Liao et al., 2016) and neurological disease (Martinez et al., 2016). RNA binding motifs (RBMs) are members of the RBP family, and have one or more RNA recognition motif (RRM) domains which partially determine their mRNA target specificity (Ray et al., 2013). In addition, RBMs regulate mRNAs in a tissue specific manner (Cirillo et al., 2014).

RNA binding motif 5 (RBM5) is a pro-death RBP that is frequently deleted in carcinomas (Kok et al., 1997). It promotes apoptosis in cancer cells by altering expression of cell death genes (Mourtada-Maarabouni et al., 2006), and also by modulating exon splicing of targets such as capase-2 (Fushimi et al., 2008), cellular flice like inhibitory protein (Bonnal et al., 2008, Jackson et al., 2015), Fas receptor (Bonnal et al., 2008), activation induced deaminase (Jin et al., 2012), and NUMB (Bechara et al., 2013).

Few studies have investigated the function of RBM5 in non-cancerous cells. To date a single report elucidated RBM5 cell signaling mechanisms in normal primary cells; RBM5 dysregulation in that study, caused by a single point mutation in the second RRM domain, affected expression of genes in the testis (including genes involved in the regulation endocytosis), and caused male sterility due to spermatid apoptosis in mice (O'Bryan et al., 2013).

RBM5 expression is high in brain vs. other organs (O'Bryan et al., 2013). Immunohistochemical staining of RBM5 in fixed *in vitro* CNS cultures or in brain tissue sections suggests that it is abundant in neuronal nuclei (Jackson et al., 2015). We reported that RBM5 protein levels increase after hippocampal/cortical injury in a mouse model of traumatic brain injury (TBI) (Jackson et al., 2015). RBM5 protein levels also increase after spinal cord trauma (Zhang et al., 2015).

Elucidation of RBM5 regulated cell signaling pathways in primary neurons is critical for understanding how changes in its expression affects neuronal function(s). Here we utilized

lentivirus mediated RNA interference (RNAi) plus gene microarray to screen for novel RBM5 cell signaling targets in primary rat cortical neurons. This report shows that RBM5 knockdown (KO) increases Rab4a mRNA/protein vs. controls, whereas RBM5 overexpression has no effect on Rab4a mRNA/protein vs. controls. Rab4a is involved in protein trafficking and endocytosis (Stenmark, 2009). Thus we measured changes in the membrane levels of its well-known target the serotonin transporter (SERT); Specifically, Rab4a has been shown to prevent translocation of SERT into the membrane by its sequestration intracellularly (Ahmed et al., 2008). As expected, increased Rab4a levels in RBM5 KO neurons were associated with decreased oligomeric SERT membrane levels. In addition, we also show that monomeric SERT uptake from plasma membrane into the cytoplasm is increased in KO vs. control neurons. More studies are needed to clarify if that effect is mediated by Rab4a or rather by an unknown gene target.

EXPERIMENTAL PROCEDURES

Chemicals & Reagents

Gibco/Life Technologies (Grand Island, NY, USA): Opti-MEM, hanks balanced salt solution (HBSS), Neurobasal/B27, Phosphate Buffered Saline (Cat#10010-023), SIGMA (St. Louis, MO, USA): Magnesium Chloride (MgCl2), Calcium Chloride (CaCl2), Sodium Chloride (NaCl), sodium bicarbonate (NaHCO3), 4-(2-hydroxyethyl)-1-piperazineethanesulfonic acid (HEPES), L-Glutamic acid, Poly-D-Lysine, chloramphenicol, TOCRIS (Bristol, UK): Fluoxetine Hydrochloride, Paroxetine Maleate, Venlafaxine Hydrochloride, Metformin Hydrochloride. Thermo Fisher Scientific (Pittsburgh, PA, USA): Dimethyl sulfoxide (DMSO), Fetal bovine serum, RNaseZap, TRIzole, linear acrylamide, 5M ammonium acetate, 2-propanol, dithiothreitol (DTT), Penicillin-Streptomycin, leupeptin hemisulfate, sulfo-NHS-SS-biotin, sulfo-NHS-biotin, radio immunoprecipitation assay (RIPA) buffer, ethylenediaminetetraacetic acid (EDTA), Glutathione, Neutravidin beads. Antibodies: Abcam (Cambridge, MA, USA) Rabbit Monoclonal [EPR12735] Anti-SERT (Cat# ab181034), Rabbit Monoclonal [EPR3042] Anti-Rab4 (Cat# ab108974), Rabbit Monoclonal [EPR7587B] Anti-Rab11A (Cat# ab128913), Rabbit Monoclonal [EPR14873] Anti-Rab8A (Cat# ab188574), Cell Signaling Technology (Danvers, MA, USA) Rabbit Monoclonal [D5A7] Anti-biotin (Cat# 5571), Rabbit Polyclonal Anti-Sec23a (Cat# 8162), Rabbit Polyclonal Anti-α-Tubulin (Cat# 2144), Atlas Antibodies (Stockholm, Sweden): Rabbit Polyclonal Anti-RBM5 (Cat# HPA018011), SIGMA: Mouse Polyclonal Anti-Rab4 (Cat# SAB1406360).

Animals

Animal work was approved by the Institutional Animal Care and Use Committee of the University of Pittsburgh. Euthanasia protocols follow recommendations established by the American Medical Veterinary Association Guidelines for Euthanasia. Sprague Dawley rats were purchased from Charles River. Timed pregnant rats were given food and water ab libitum and maintained on a 12h light/dark cycle. Embryos were harvested at ~E16-E17.

Primary Cortical Neuron Culture

Mixed male/female cortical neurons were pooled and cultured using our standard protocol. In brief, tissues were harvested under a dissecting microscope (M651 light microscope, Leica; Buffalo Grove, IL, USA) in hanks balanced salt solution (HBSS) supplemented with 15mM HEPES, 10mM sodium bicarbonate, and 100U/mL penicillin-streptomycin. Neural tissue was trypsinized 8min/37°C, quenched in Neurobasal/B27/10%FBS, centrifuged 5min/200g/4°C, and resuspended in trituration media. Tissue was disassociated by trituration (10 times) through a fire-polished glass pasteur pipette. Cells were centrifuged 5min/200g/4°C and resuspended in Neurobasal/B27 media supplemented with 100U/mL penicillin-streptomycin and 25μM L-Glutamic acid. Neurons were counted on a Cellometer (Nexcelom Bioscience; Lawrence, MA, USA), and transduced at DIV0 (i.e. time of plating) with 30–60 multiplicity of infection (MOI) lentivirus. Neurons used for RNA extraction experiments were seeded onto 10cm dishes at a density of 5×10^6. Neurons used for protein analysis and endocytosis experiments were seeded onto 6-well plates at a density of 1.2×10^6. Plastic ware was coated overnight with Poly-D-Lysine (0.05mg/mL) prior to seeding. Neurons were maintained by ½ media exchange every 3d and used for experiments on DIV3-DIV12.

RNA Extraction

Labware and table tops were cleaned with RNaseZap. DIV6 neurons (10cm dishes) were transferred from a 37°C/5% CO_2 incubator and immediately put on ice. Cells were washed twice with freshly prepared 1mM DTT dissolved in ice cold RNase free PBS. Final PBS wash was replaced with 1mL TRIzole (under a chemical fume hood). Cells were quickly scraped off dishes and extracts transferred into 1.5mL RNase free polypropylene tubes. Extracts were pipetted up/down 10–15 times, centrifuged 14,000rpm/10min/4°C (to remove debris), and transferred into new 1.5mL tubes. 200μL chloroform was added to samples then vigorously shaken 15s and incubated at room temperature for 10min. Samples were spun 14,000rpm/15min/4°C. The aqueous (RNA containing) phase was transferred into a new tube and mixed with 6μL linear acrylamide, 60μL 5M ammonium acetate, and 600μL of 2-propanol. Tubes were inverted 30 times then incubated 1h in a −20°C freezer. Samples were spun at 14,000rpm/10min/4°C. Supernatants were carefully removed so as not to disturb RNA pellets. 1mL 80% RNase free ethanol (prepared in RNase free water) was added into tubes. Pellets were washed a total of three times; each wash included pipetting RNA pellets up/down 15 times using a 1mL pipette tip, followed by 15 tube inverts, and centrifugation at 10,000rpm/5min/4°C. After removal of the last ethanol wash, tubes were given a final brief spin (70s/10,000rpm/4°C) to remove excess alcohol adhering to the tube wall. Pellets were air dried under a laminar flow hood and resuspended in 25μL RNase free water. Total RNA concentrations and validation of ultra-pure RNA (Fig. 1A) was confirmed using a Genova Nano (JENWAY; Staffordshire, UK). Samples were stored at −80°C.

Microarray Analysis

A total of 14 Clariom™D/GeneChip® Rat Transcriptome Array 1.0 (RTA 1.0.) microarrays were purchased from Affymetrix (Santa Clara, CA, USA), and used to measure gene expression in RBM5 KO and overexpressing neurons vs. controls (See Study Design, Fig. 1B). The GeneChip® WT Plus reagent kit was used to prepare cDNA following

manufacturer instructions. In brief, reverse transcription was performed on 100ng total RNA and dNTP-T7 random primers. Amplified cRNA was made using second strand synthesis and in vitro transcription. cDNA was produced by a subsequent reverse transcription and then fragmented. Fragments were biotin end-labeled in preparation for hybridization to the RTA. The Affymetrix GeneChip® Hybridization, Wash, and Stain kit was used for array processing. 5.2μg biotin-labeled fragmented ss-cDNA was added to 1× hybridization buffer containing oligo B2, hybridization controls, and DMSO. Following incubation at 95°C and 45°C for 5 minutes each, 200μL hybridization mix was loaded onto each array. Arrays were incubated for 16h in a GeneChip 645 hybridization oven (Affymetrix) at 45°C with rotation at 60rpm. Wash/stain procedures were performed on an Affymetrix 450 Fluidics Station using manufacturer specified instrument protocol settings. To remove unbound sample, arrays were washed with non-stringent wash-Buffer A. GeneChips® were then stained 10min in Stain cocktail 1. Excess stain was removed by subsequent wash in Buffer A. Arrays were incubated 10min with Stain Cocktail 2 followed by 10min incubation with Stain Cocktail 1 for signal amplification. GeneChips were washed with Buffer B then filled with Array Holding Buffer prior to removal from the fluidics station, and scanned using the GeneArray® 3000 scanner (Affymetrix). Results were normalized by robust multi-array average (RMA). First level data analysis was done in Affymetrix Expression Console software and subsequently in Transcriptome Analysis Console (TAC). The data discussed in this publication have been deposited in NCBI's Gene Expression Omnibus (Edgar et al., 2002) and are accessible through GEO Series accession number GSE98858 (https://www.ncbi.nlm.nih.gov/geo/query/acc.cgi?acc=GSE98858).

Real-Time *PCR*

Total RNA was reversed transcribed using the High Capacity cDNA kit (Thermo Fisher Scientific), according to manufacturer directions. 2× master mix containing 5 U/μL multiscribe reverse transcriptase was prepared from kit components of 10× reverse transcription buffer, 10× random primers, 25× dNTP mix, and 50 U/μL multiscribe reverse transcriptase. Equal volumes of 2× master mix and total RNA sample containing 1 μg were mixed and incubated in a thermocycler for 10min at 25°C followed by 2h at 37°C. Reaction was held at 4°C and then frozen at −20C until PCR set up. Realtime PCR was carried out using Gene Expression PCR master mix (Thermo Fisher Scientific) at 1× concentration containing 125 nM of each primer and 50 ng cDNA product. Rat gene specific TaqMan (FAM-MGB) primers were purchase from Thermo Fisher Scientific (GAPDH, Rn99999916_s1, Cat# 4453320; Sec23a, Rn01472992_m1, Cat#4448892; Rab4a, Rn01426714_m1, Cat#4448892). Taq activation step of 12min at 95°C was followed by 40 cycles of 15s at 95°C and 1min at 60°C. Data analysis was performed using SDS 2.4 (ThermoFisher Scientific) with automatic baseline and Ct threshold. Delta Ct was calculated against the endogenous control (GAPDH).

Bacterial Transfections & DNA Plasmid Amplification

Expression plasmids were reconstituted in sterile ddH_2O (0.1μg/μL). DNA transformations were done using Alpha-Gold Competent E.coli (Origene; Rockville, MD, USA). 5μL expression plasmid was mixed with 50μL E.coli in pre-chilled 14mL round bottom tubes, incubated 30min on ice, subjected to 45s heat shock via 42°C water bath, returned on ice for

2min, and the reaction mix diluted in 945μL super optimal broth (SOC) media. Tubes were shaken 1h/200rpm/37°C. Transformed E.coli were streaked onto Luria-Bertani (LB)-agar plates containing 34μg/μl chloramphenicol and incubated overnight at 37°C. Chloramphenicol resistant bacterial colonies were isolated using sterile pipet tips and shaken 8h/250rpm/37°C in 3mL LB-medium (containing 34μg/μL chloramphenicol). 6μL of media (containing exponentially dividing cells) was diluted into 3mL of fresh LB containing 34μg/μL chloramphenicol and shaken overnight/250rpm/37°C. 1.5mL of bacterial containing growth media was diluted into 300mL fresh LB plus 34μg/μL chloramphenicol and shaken overnight/ 200rpm/37°C. The Qiagen EndoFree Plasmid Maxi Kit (Qiagen; Germantown, MD, USA) was used for DNA plasmid purification. Transformed bacteria were pelleted by 15min/3000g/4°C centrifugation. Pellets were resuspended in buffer, lysed, and filtered to remove proteins, genomic DNA, and detergent. Lysate wash buffer was used to remove contaminants. Plasmid DNA was eluted into sterile 50mL polypropylene centrifuge tubes. Isopropanol precipitation of DNA was done at room temperature then pelleted by 1.5h/3000/4°C centrifugation. The supernatant was carefully removed, DNA pellets washed in endotoxin-free 70% ethanol, given a final 1h/3000g/4°C centrifugation, air dried at room temperature, and reconstituted in TE buffer. High-quality amplified plasmids were stored at −20°C. DNA concentrations and purity were confirmed by UV spectrophotometry.

High-Titer Lentivirus

Biosafety level 2 experiments were approved by the University of Pittsburgh Institutional Biosafety Committee. Lentivirus expression vectors were purchased from Origene: pLenti-C-Myc-DDK (Empty Control Vector, Cat# PS100064), pLenti-C-Myc-DDK-RBM5_ORF (Cat# RR213857L1), pGFP-C-shLenti (non-targeting shRNA control, Cat# TR30021), pGFP-C-shLenti (RBM5 targeting shRNA #1, TL704115A), pGFP-C-shLenti (RBM5 targeting shRNA #2, TL704115B), pGFP-C-shLenti (RBM5 targeting shRNA #3, TL704115C), pGFP-C-shLenti (RBM5 targeting shRNA #4, TL704115D). Packaging plasmids were purchased from Origene (Cat# TR3002P5). Expression plasmids were maxi-prepped prior to transfection into HEK293Ta cells (Genecopoeia; Rockville, MD, USA). In brief, HEK293Ta cells (grown in T225 culture flasks) were transfected over 12h with lentiviral packaging plasmids, expression plasmids, and MegaTran transfection reagent in Opti-MEM/10%FBS/Penicillin-Streptomycin. Supernatant was harvested at ~36h and 48h post-transfection. Lentivirus containing culture media was passed through a 0.45micron Nalgene-membrane and concentrated using Centricon® Plus-70 Centrifugal Filter Units. Viral supernatant was further concentrated by ultra-centrifugation 1.5h/24,000rpm/4°C in a XL-90 Beckman Ultracentrifuge (Beckman-Coulter; Indianapolis, IN, USA). Viral pellets were resuspended overnight in ~200μL Opti-MEM, aliquoted, and stored at −80°C. Viral concentration was measured by QuickTiter™ Lentivirus Titer Kit (Cell Biolabs Inc; San Diego, CA, USA). Overexpression vectors were used at 30 multiplicity of infection (MOI). shRNA vectors were used at 50–60 MOI (i.e. each batch tested to achieve ~90%).

Biotinylation & Endocytosis

Investigation of neuronal endocytosis was done as described by Arancibia-Carcamo L., et al with minor modification (Arancibia-Carcamo et al., 2006). Neurons requiring 30min (post-

biotinylation) study of endocytosis received 1h pretreatment with 100μg/mL leupeptin hemisulfate to inhibit endosomal degradation by lysosomes. DIV12 neurons in 6-well plates were removed from a 37°C/5% CO_2 incubator and immediately put on ice to block endocytosis. Conditioned Neurobasal/B27 growth media (CM) was discarded in experiments measuring only total labeling of plasma membrane biotinylation. In contrast, in endocytosis studies, CM was immediately collected, separated by vector-specific manipulations in 15mL tubes (NT-control vs. RBM5 shRNA vs. No Virus), and mixed with fresh Neurobasal/B27 media (i.e. 2/3 CM and kept in a 37°C water bath). Neurons were twice washed with ice-cold PBS supplemented with 0.5mM MgCl2 and 1mM CaCl2 (sPBS). Sulfo-NHS-biotin (standard) or sulfo-NHS-SS-biotin (glutathione cleavable) was dissolved in sPBS (1mg/mL) and incubated on neurons for ~15min. Cells were washed three times in 50mM glycine/sPBS to quench excess biotin, followed by two additional washes in sPBS (without glycine). Protein extracts were immediately harvested in 75μL RIPA buffer (supplemented with EDTA and protease/phosphatase inhibitors), and further processed as detailed below. To induce endocytosis cells were returned to a 37°C/5% CO_2 incubator in 1mL per well 2/3 CM. A control plate treated with sulfo-NHS-SS-biotin and given CM exchange remained on ice; after the 30min incubation half the plate (n=3) received glutathione stripping (as described below). Control samples estimate maximum biotinylation as well as the efficiency of glutathione stripping to remove plasma membrane biotin. After the 30min endocytosis incubation period, 2/3 CM media was discarded and sulfo-NHS-SS-biotin cleavage initiated by two 15min washes in 50mM (freshly prepared) glutathione dissolved in sPBS (and further supplemented with 75mM NaCl, 10mM EDTA, and pH adjusted to ~7.8–8.0). Three additional washes in sPBS removed any remaining glutathione. Protein extracts were harvested in 75μL RIPA buffer supplemented with EDTA and protease/phosphatase inhibitors. Samples (in 0.6mL tubes) were rotated ~1h in a 4°C cooler, centrifuged 14,000g/15min/4°C, supernatants collected and transferred into new tubes, and mixed with 200μL Neutravidin bead slurry (which had been pre-washed by three equal volume exchanges in sPBS to remove storage solution). Bead/extract mix was rotated 2h in a 4°C cooler, and centrifuged 5,000rpm/1min/4°C. The supernatant was collected and stored at −80°C (Cytoplasmic/nuclear fraction). Biotin bound beads were resuspended and washed twice in 500μL RIPA buffer supplemented with 500mM NaCl. A final wash was given in 500uL RIPA (without NaCl) and samples centrifuged 1min/5,000rpm/4°C. Beads were resuspended in 40μL Laemmeli sample loading buffer and stored at −80°C. In preparation for Western blotting, 2-mercaptoethanol (1:20) was added to thawed biotinylated protein samples, vortexed, boiled 95°C/5min, immediately centrifuged 15min/16,000g/4°C, and ~42μL supernatant loaded onto 10 well (50μL/well) precast gels.

Antidepressants & Metformin Drug Treatments

Drug treatments were started on DIV6. Fluoxetine, Paroxetine, and Venlafaxine were dissolved in DMSO. Drugs were diluted into maintenance media on DIV6 and on DIV9, and applied at a final concentration of 1μM. Antidepressant dose was chosen based off work by Cecconi D. and colleagues (Cecconi et al., 2007). Controls received an equal volume of DMSO (~0.25%). Metformin was diluted in double-distilled sterile water (ddH_2O) and also administered on DIV6/DIV9 during ½ media exchanges. All Metformin doses (as well as controls) received equal volume ddH_2O.

Western Blot

Gel electrophoresis was done using our standard protocol. In brief, neuron extracts were sonicated 20–30s, centrifuged 15min/16,000g/4°C, and protein homogenate concentrations determined by bicinchoninic acid (BCA) method (Thermo Fisher Scientific). 5–20μg protein was loaded onto 4–15% gradient SDS-PAGE TGX™ precast gels (BioRad; Hercules, CA, USA). Samples were electrophoresed, transferred to Amersham Hybond P 0.2 PVDF membrane (GE Healthcare Bio-Sciences; Pittsburgh, PA, USA), and blocked 1h in tris buffered saline (TBS) supplemented with 0.1% tween-20 (TBST). Neutravidin-captured biotinylated proteins, which are not amendable to classical protein loading controls, were stained with (reversible) Swift Membrane Stain™ (Thermo Fisher Scientific) prior to blocking (which has a detection limit of 0.5ng). Blots were incubated in primary antibodies diluted in TBST at 4°C overnight on a rocker. Blots were washed three times in TBS, incubated with secondary antibody (in TBST) for 2h, washed three additional times in TBS, incubated ~1.5min in ECL-2 Substrate (Thermo Fisher Scientific), films developed in a dark-room, and TIFF images captured on a 600dpi flatbed scanner. Figures were compiled in Photoshop (Adobe; San Jose, CA, USA).

Statistical Analysis

Samples from three (n=3 NT-shRNA vs. n=3 RBM5 KO) or four (n=4 empty vector vs. n=4 RBM5 ORF) independent experiments (i.e. different neuronal cultures prepared from different rats on different days) were analyzed by microarray. CEL expression files were imported into Expression Console (Affymetrix) for gene-level normalization and signal summarization. Resulting CHP files were analyzed in TAC (Affymetrix). Gene comparisons were analyzed using unpaired 1-Way-ANOVA ($p<0.05$) followed by false discovery rate (FDR) correction using Benjamini-Hochberg Step-Up FDR-controlling Procedure (alpha set to 0.05). Dendrogram shows significant gene changes by 1-Way-ANOVA (prior to FDR correction). RT-PCR data was analyzed by comparative Ct method ($2^{-\Delta\Delta Ct}$) to determine relative gene expression of Rab4 and Sec23a. GAPDH was used as the internal control. NT-virus control samples were used as the calibrator. Fold change ($2^{-\Delta\Delta Ct}$) was analyzed by an unpaired T-test (three-four independent experiments). Western blot data were analyzed in GraphPad PRISM by unpaired T-test or 1-Way ANOVA followed by Newman-Keuls post-hoc test. (GraphPad Software Inc, La Jolla, USA). Graphs show mean + SEM. Data is significant at $p<0.05$.

RESULTS

Analysis of Gene Expression in RBM5 KO and Overexpressing Primary Rat Cortical Neurons

Rat cortical neurons were transduced with lentivirus to deliver either a non-targeting-shRNA (NT), an RBM5 targeting shRNA (KO), empty overexpression vector (Empty Vector), or rat specific DDK-tagged RBM5 (RBM5 ORF). High-purity total RNA extracts were isolated on day in vitro 6 (DIV6) (Fig. 1A). A separate plate of cells was harvested for protein analysis, to confirm RBM5 KO vs. overexpression, and also to verify protein changes in potential mRNA targets discovered by microarray (Fig. 1B). RBM5 shRNA induced ~90% protein

KO in three independent experiments (Condition 1; Fig. 2A, and 2C). RBM5 ORF increased protein levels ~2-fold above baseline (Condition 2; Fig. 2B, and 2D).

Condition 1 caused 305 gene changes before FDR correction. 102 genes were up-regulated in RBM5 KO vs. control neurons (70 coding genes, 11 non-coding, 21 unassigned); 204 genes were down-regulated (45 coding, 97 non-coding, 57 unassigned, 1 complex, and 4 pseudogenes). In total there were 115 possible coding gene differences (Fig. 3A).

Condition 2 caused 5 gene changes before FDR correction. 4 genes were up-regulated in RBM5 ORF vs. control neurons (2 coding genes, 2 non-coding) and 1 non-coding gene was down regulated. In total, 2 coding genes were upregulated; RBM5 (ANOVA p=<0.0001, FDR corrected p=0.175) and predicted gene 11096 (ANOVA p=0.042, FDR corrected p=0.999).

We focused downstream efforts on the two highest scoring genes identified in Condition 1 (Fig. 3B); Sec23a (ANOVA p=<0.0001, FDR corrected p=0.069) and Rab4a (ANOVA p=<0.0001, FDR corrected p=0.069). Quantitative real-time PCR (qPCR) was done on the same RNA samples used for microarray. Both Rab4a and Sec23a mRNA were significantly increased (~2-fold) in RBM5 KO neurons vs. non-targeting controls (Fig. 3C, D, and E).

Analysis of Rab4a Protein Levels

Rab4a protein levels significantly increased in KO neurons in three independent experiments vs. non-targeting controls (Fig. 4A and B). Two different anti-Rab4 antibodies were used to validate increased Rab4a protein levels (A mouse polyclonal anti-Rab4 antibody Fig. 4C and D, and a rabbit monoclonal anti-Rab4 antibody Fig. 4E and F). Rab4a levels were low in NT control neurons. In contrast, Rab4a protein increased as early as DIV3 in RBM5 KO neurons relative to controls, and levels were highest by DIV12 (Fig. 4C–F). Cells were harvested at the DIV12 time point in subsequent KO experiments (Fig. 5, 6, and 7).

In an independent experiment, Sec23a protein levels were not significantly different in RBM5 KO vs. control neurons (Fig. 5A and B). Similarly, there were no significant group differences in protein levels of other Rab proteins including Rab8a (Fig. 5A and D) or Rab11a (Fig. 5A and E). However, Rab4a significantly increased as expected (Fig. 5A, and C). Increased Rab4a was not due to off-target effects of the exon 12 targeting RBM5 shRNA as three additional RBM5 targeting shRNAs also increased Rab4a protein levels vs. control (Fig. 5I and J). Contrary to expectations, in DIV6 neurons, RBM5 overexpression did not decrease protein levels of Rab4a (Fig. 5F) nor did it decrease mRNA levels of Sec23a (Fig. 5G) or Rab4a (Fig. 5H).

Analysis of Membrane Localized SERT

We used a standard biotin assay to isolate and measure membrane levels of SERT in neurons (Arancibia-Carcamo et al., 2006). Biotin was covalently linked to extracellular membrane proteins in NT and KO neurons. Neutravidin isolated proteins (i.e. which are separated from other subcellular proteins using the biotin tag) were analyzed by Western blot. Reversible membrane stain shows different staining patterns comparing biotinylated membrane extracts vs. cytoplasmic/nuclear extracts (Fig. 6A). Biotinylated extracts contain captured membrane

proteins as well as ~60 kDa Neurtavidin and its breakdown products. Anti-biotin antibody shows enrichment of high-molecular weight neuronal transmembrane proteins in membrane extracts, and also confirms the absence of signal in cytoplasmic/nuclear fractions (Fig. 6B). Oligomeric SERT membrane levels were decreased by ~78% in RBM5 KO neurons vs. NT controls (Fig. 6C, D). Monomeric SERT was detected in cytoplasmic/nuclear fractions but not in membrane fractions (Fig. 6C, bottom blot showing 10min exposure). Cytoplasmic/nuclear extracts (from cells used to isolated biotin membrane fractions) were probed with anti-RBM5 and anti-Rab4 antibodies to confirm KO, and also confirm increased Rab4a (Fig. 6E).

Next we tested if SERT uptake was directly affected in RBM5 KO neurons vs. controls. We repeated the biotinylation study with two key modifications (Fig. 7): (I) cells were given 1h pre-treatment with a lysosomal inhibitor (before biotinylation) to prevent rapid degradation of internalized plasma membrane derived proteins, and (II) membrane proteins were covalently modified with a glutathione-cleavable biotin substrate. This was used to remove biotin membrane protein labeling, except from internalized proteins, which are protected from non-cell permeable glutathione.

Control experiments were done to validate the conditions used to study SERT uptake/endocytosis in our protocol. Samples in three groups were all treated with cleavable biotin. *MAX-Biotin* samples were left on ice (preventing endocytosis) and did not receive a glutathione strip. *Cnt-Strip* samples were left on ice (preventing endocytosis) and received glutathione treatment/strip (to confirm removal of biotin from labeled membrane proteins). *Cnt-30min Endo* samples were biotinylated, returned to a 37°C incubator (to initiate endocytosis and/or other mechanisms of protein uptake), and afterwards received glutathione treatment/strip to remove any remaining extracellular membrane biotin. Neutravidin isolated proteins were analyzed by Western blot and total protein stain examined (Fig. 7A). As expected, total protein stain showed decreased signal in samples subjected to a glutathione strip (Fig.7A)

Monomeric ~70kDa SERT was detected in all three treatment groups at the expected variations in levels (Fig.7B, *MAX-Biotin, Cnt-Strip* and *Cnt-30min Endo*). Of note, monomeric SERT was not detected in Fig. 6 experiments, in which we did not include a lysosomal inhibitor. Thus, in our hands, inhibition of protein degradation appears vital for detection of monomeric SERT in membrane-derived fractions, which is in agreement with reports that membrane-internalized SERT is rapidly targeted to lysosomes (McCaffrey et al., 2001, Rahbek-Clemmensen et al., 2014). Finally, oligomeric SERT was not detected in samples given a glutathione strip (Fig. 7B, *Cnt-Strip* and *Cnt-30min Endo*), which suggests it was not internalized (at least during the brief 30min endocytosis period studied here). We next compared the uptake of ~70kDa SERT after a 30min endocytosis period in RBM5 KO vs. NT control neurons. Total protein stain of Neutravidin isolated proteins did not differ by genotype (Fig. 7C). RBM5 KO neurons had a ~413% increase in monomeric SERT uptake/endocytosis relative to controls (Fig. 7D, E). Cytoplasmic/nuclear extracts were probed with anti-RBM5 and anti-Rab4 antibodies to confirm KO, and also increased Rab4a in samples (Fig. 7F).

Chronic Treatment of Cortical Neurons with SSRIs or Metformin Does not Alter Rab4a or RBM5 Levels

Preventing or reversing decreased Rab4 levels may have therapeutic significance in conditions like depression (Kang et al., 2012). In a literature review we identified selective serotonin reuptake inhibitors (SSRIs) and metformin as the only class of clinically used compounds that (to the best of our knowledge) reportedly increase Rab4a levels in cells. Because the mechanism of Rab4a induction by these agents is unclear, we tested if they might decrease RBM5 levels. 1μM fluoxetine has previously been shown to alter proteins after 3d in cultured rat cortical neurons (Cecconi et al., 2007). DIV6 cortical neurons were given 1μM fluoxetine, paroxetine, or venlafaxine for a total of 6d and subsequently harvested at DIV12 for protein analysis (Fig. 8A, B, C). In our hands none of the antidepressants, at doses tested here, increased Rab4a levels. Furthermore, antidepressants did not affect RBM5 levels (Fig. 8A, B, C).

10mM metformin reportedly increases Rab4a in mouse myoblast C2C12 cells (Lee et al., 2012). In pilot studies we were unable to replicate similar treatment conditions because 10mM metformin led to complete neuronal cell death within days. Similarly, 1mM metformin also markedly reduced neuron viability by 6d (pH change indicated by yellow media in phenol red containing Neurobasal across time, suggests that severe acidosis may have been the cause of neuronal death). However, 6d treatment with 1–100μM metformin was tolerated in cortical neurons but did not increase Rab4a levels nor alter RBM5 (Fig. 8D).

DISCUSSION

Rab4a Levels are increased in RBM5 KO Neurons

Here we show that Rab4a levels are increased in RBM5 KO neurons vs. controls using microarray, qPCR, and Western blot. The small GTPase Rab4a is involved in endosomal trafficking (Stenmark, 2009). Large-scale transcriptome analysis projects by others have similarly reported RBM5-dependent changes in the expression of endocytosis regulators including Rab37 (O'Bryan et al., 2013, Loiselle et al., 2016). Thus our findings add support to the hypothesis that RBM5 is involved in the regulation of endocytosis – although more work is needed to confirm that conclusion in neurons.

Future studies are also needed to elucidate the mechanism(s) by which RBM5 regulates Sec23a and Rab4a levels. RBM5 is a well-known splicing factor (Fushimi et al., 2008, Bechara et al., 2013). It is possible that RBM5 KO directly effects Rab4a splicing, which might give rise to variants that have altered mRNA stability and/or altered rates of protein degradation (van der Lee et al., 2014). However, contrary to that notion, Gene Ensemble predicts a single mRNA encoded by the rat Rab4a gene (i.e. the species studied here). Thus it is presently unclear if Rab4a splicing occurs in the rat. By contrast, the human Rab4a gene has 5 predicted splice variants (two protein coding variants and three non-coding variants). Future studies also need to test if RBM5 regulates Rab4a expression similarly or differently in human neuronal cells (in which splicing mechanisms may differ).

Indirect mechanisms may also play a role in altered cell signaling pathways observed here. Increased Rab4a may be compensatory to alterations in other components of the endocytic pathway. There are over 60 Rab proteins that are intricately linked together and which orchestrate endosomal trafficking (Pfeffer and Aivazian, 2004). Future studies should analyze the entire endocytic pathway at the protein level in RBM5 KO neurons, which might reveal additional targets potentially altered by KO that contribute to increased Rab4a expression and that were undetected by microarray.

Unexpectedly, RBM5 overexpression did not decrease in Rab4a levels (mRNA or protein). Several factors could have contributed to the apparent lack of an effect by RBM5 overexpression. First, we targeted RBM5 levels to ~2-fold above baseline because it approximates increases in protein levels that we have seen after injury *in vivo*. However, moderate RBM5 overexpression (i.e. ~2-fold) may be insufficient to alter gene expression. Furthermore, RBM5 protein appears to be considerably higher (~3–4 fold above sham) after SCI *in vivo* or H_2O_2 injury to PC12 cells *in vitro* (Zhang et al., 2015). Thus viral dose-response studies are needed to test the effect of increasing RBM5 levels (by overexpression) on gene changes as measured by microarray or RNA-seq.

Secondly, we did not injure primary neurons. This is the first study to search for novel RBM5 targets in primary neurons. Therefore we felt it logical to simplify experiments by investigating changes in normal/healthy cells. However, increased RBM5 levels may be physiologically relevant in the injury setting, and could preferentially regulate certain mRNAs only (or primarily) expressed in the injury milieu (e.g. such as caspase-2 which increases after brain ischemia and is also targeted by RBM5 in cancer cells (Jin et al., 2002, Fushimi et al., 2008).

Finally, a lack of an effect of RBM5 overexpression (on Rab4a levels) adds support to the notion that indirect mechanisms may play a bigger role in mediating the increase in Rab4a in KO neurons (rather than a direct effect on mRNA stability and/or splicing). Also, because RBM5 is a component of the early spliceosomal complex, its ablation by KO may cause broader changes on cell signaling pathways in uninjured neurons vs. mild overexpression which may be comparatively benign. (Mourao et al., 2016).

SERT Membrane Levels are decreased in RBM5 KO Neurons

Rab4a regulates protein trafficking in neurons, and promotes degradation of select proteins (van der Sluijs et al., 1992, McCaffrey et al., 2001). SERT is a well-known Rab4a target (Ahmed et al., 2008, Rahbek-Clemmensen et al., 2014, Rajamanickam et al., 2015). Rab4a co-immunoprecipitates with SERT in blood platelets, and decreases membrane SERT levels by sequestering it intracellularly (Ahmed et al., 2008).

Monomeric SERT (endosomal-derived and cytoplasmic) migrates at ~68–75kDa on SDS gel electrophoresis (Zhu et al., 2011, Rahbek-Clemmensen et al., 2014). Membrane localized SERT is oligomeric (active form) and migrates from 130–180kDa under reducing conditions (Jess et al., 1996, Zhu et al., 2011). Consistent with observations by others, we found that oligomeric SERT is detected in biotinylation-NeutrAvidin isolated (total) plasma membrane

extracts. As expected, SERT total membrane levels were decreased in RBM5 KO neurons which had higher Rab4a levels vs. controls.

We also tested if RBM5 KO might directly alter SERT uptake/removal from the membrane (potentially due to increased endocytosis). Intriguingly, membrane-derived intracellular monomeric SERT was increased in RBM5 KO neurons relative to controls. This suggests that increased SERT uptake may be another mechanism partially contributing to decreased membrane levels in neurons (in addition to Rab4a-dependent SERT sequestration). However, we cannot rule out the possibility that other genes affected by RBM5 KO (besides Rab4a), might be responsible for increased SERT uptake in neurons.

Neurobiological Implications

RBM5 dependent changes in Rab4a or SERT levels may have neurobiological implications, although more studies are needed to confirm that this regulation also occurs *in vivo*. Germane to Rab4, it is known to regulate (I) constitutive endocytosis of dopamine D2 receptors in striatal medium spiny neurons (Li et al., 2012), (II) is critical for the maintenance of dendritic spine size in rat hippocampus (Brown et al., 2007), (III) promotes elongation/growth of developing Xenopus retinal axons (Falk et al., 2014), (IV) is a key binding partner of GRIP-associated protein-1 (GRASP-1) which facilitates AMPA receptor recycling in primary hippocampal neurons (Hoogenraad et al., 2010), and (V) is activated by acute stress and promotes NMDAR/AMPAR glutamatergic neurotransmission which enhances working memory in rodents (Yuen et al., 2011).

SERT on the other hand is altered in many psychiatric disorders/CNS diseases such as Alzheimer's disease (Thomas et al., 2006), Parkinson's disease (Pagano et al., 2016), schizophrenia (Laruelle et al., 1993), autism (Nakamura et al., 2010), anxiety (Sakakibara et al., 2014), alcoholism/drug addiction (Storvik et al., 2008), memory disturbances (Meneses et al., 2011), and in depression (Kambeitz and Howes, 2015). Germane to the latter, Rab4 is also a target in depression; Rab4b is among synaptic proteins decreased in prefrontal cortex of patients with major depressive disorder (Kang et al., 2012). Large-scale proteomic studies in rats indicate that SSRIs increase Rab4 levels in brain tissue (Khawaja et al., 2004). We tested if SSRIs might potentially decrease RBM5 levels (i.e. a contributing mechanism mediating Rab4 upregulation). In our hands, 6d treatment of neurons with 1μM fluoxetine, paroxetine, or venlafaxine did not alter Rab4a or RBM5 levels (Fig. 8). The anti-diabetic agent Metformin increases Rab4a levels in mouse myoblast C2C12 cells (Lee et al., 2012) but does not appear to have the same effect in primary rat cortical neurons.

In summary, here we show that RBM5 KO is associated with altered Rab4a and SERT homeostasis in primary rat neurons. Given that endogenous mechanisms exist by which RBM5 activity could be decreased in humans - such as by microRNAs (miRNA) (Selbach et al., 2008), intronic antisense transcripts located within the RBM5 precursor mRNA (e.g. Je2) (Mourtada-Maarabouni et al., 2002, Rintala-Maki and Sutherland, 2009), other long non-coding RNAs (lncRNA) (Sehgal et al., 2014), and by RBM5 polymorphisms (Oh et al., 2007) - future studies are needed to examine if RBM5 similarly regulates Rab4a/SERT in human neurons.

Acknowledgments

This work was supported by NIH/NINDS grant R21NS088145 to Travis C. Jackson. This project used the University of Pittsburgh HSCRF Genomics Research Core microarray analysis and real-time PCR services. The content is solely the responsibility of the authors and does not necessarily represent the official views of the National Institutes of Health.

Travis. C. Jackson and Patrick M. Kochanek are inventors on USPTO Patent No. 9,610,266 titled, “Small Molecule Inhibitors of RNA Binding Motif (RBM) Proteins for the Treatment of Acute Cellular Injury”.

ABBREVIATIONS

RBM5	RNA binding motif 5
KO	Knockdown
Rab4	Ras-related protein Rab-4
Sec23a	Protein Transport Protein Sec23A
SERT	Serotonin Transporters
RBPs	RNA Binding Proteins
RBMs	RNA Binding Motifs
RRM	RNA Recognition Motif
NUMB	NUMB, endocytic adaptor protein
TBI	Traumatic Brain Injury
SCI	Spinal Cord Injury
RNAi	RNA Interference
shRNA	Short-Hairpin RNA
GRASP-1	GRIP-Associated Protein-1
NMDAR	N-methyl-D-aspartate receptor
AMPAR	α-amino-3-hydroxy-5-methyl-4-isoxazolepropionic acid receptor
lncRNA	Long Non-Coding RNAs
SSRIs	Selective Serotonin Reuptake Inhibitors

References

Ahmed BA, Jeffus BC, Bukhari SI, Harney JT, Unal R, Lupashin VV, van der Sluijs P, Kilic F. Serotonin transamidates Rab4 and facilitates its binding to the C terminus of serotonin transporter. The Journal of biological chemistry. 2008; 283:9388–9398. [PubMed: 18227069]

Arancibia-Carcamo, IL., Fairfax, BP., Moss, SJ., Kittler, JT. Studying the Localization, Surface Stability and Endocytosis of Neurotransmitter Receptors by Antibody Labeling and Biotinylation Approaches. In: Kittler, JT., Moss, SJ., editors. The Dynamic Synapse: Molecular Methods in Ionotropic Receptor Biology. Boca Raton (FL): 2006.

Bechara EG, Sebestyen E, Bernardis I, Eyras E, Valcarcel J. RBM5, 6, and 10 differentially regulate NUMB alternative splicing to control cancer cell proliferation. Molecular cell. 2013; 52:720–733. [PubMed: 24332178]

Bonnal S, Martinez C, Forch P, Bachi A, Wilm M, Valcarcel J. RBM5/Luca-15/H37 regulates Fas alternative splice site pairing after exon definition. Molecular cell. 2008; 32:81–95. [PubMed: 18851835]

Brown TC, Correia SS, Petrok CN, Esteban JA. Functional compartmentalization of endosomal trafficking for the synaptic delivery of AMPA receptors during long-term potentiation. The Journal of neuroscience : the official journal of the Society for Neuroscience. 2007; 27:13311–13315. [PubMed: 18045925]

Castello A, Fischer B, Frese CK, Horos R, Alleaume AM, Foehr S, Curk T, Krijgsveld J, Hentze MW. Comprehensive Identification of RNA-Binding Domains in Human Cells. Molecular cell. 2016; 63:696–710. [PubMed: 27453046]

Cecconi D, Mion S, Astner H, Domenici E, Righetti PG, Carboni L. Proteomic analysis of rat cortical neurons after fluoxetine treatment. Brain research. 2007; 1135:41–51. [PubMed: 17196950]

Cirillo D, Marchese D, Agostini F, Livi CM, Botta-Orfila T, Tartaglia GG. Constitutive patterns of gene expression regulated by RNA-binding proteins. Genome Biol. 2014; 15:R13. [PubMed: 24401680]

Edgar R, Domrachev M, Lash AE. Gene Expression Omnibus: NCBI gene expression and hybridization array data repository. Nucleic Acids Res. 2002; 30:207–210. [PubMed: 11752295]

Falk J, Konopacki FA, Zivraj KH, Holt CE. Rab5 and Rab4 regulate axon elongation in the Xenopus visual system. The Journal of neuroscience : the official journal of the Society for Neuroscience. 2014; 34:373–391. [PubMed: 24403139]

Fushimi K, Ray P, Kar A, Wang L, Sutherland LC, Wu JY. Up-regulation of the proapoptotic caspase 2 splicing isoform by a candidate tumor suppressor, RBM5. Proceedings of the National Academy of Sciences of the United States of America. 2008; 105:15708–15713. [PubMed: 18840686]

Glisovic T, Bachorik JL, Yong J, Dreyfuss G. RNA-binding proteins and post-transcriptional gene regulation. FEBS letters. 2008; 582:1977–1986. [PubMed: 18342629]

Hoogenraad CC, Popa I, Futai K, Martinez-Sanchez E, Wulf PS, van Vlijmen T, Dortland BR, Oorschot V, Govers R, Monti M, Heck AJ, Sheng M, Klumperman J, Rehmann H, Jaarsma D, Kapitein LC, van der Sluijs P. Neuron specific Rab4 effector GRASP-1 coordinates membrane specialization and maturation of recycling endosomes. PLoS biology. 2010; 8:e1000283. [PubMed: 20098723]

Jackson TC, Du L, Janesko-Feldman K, Vagni VA, Dezfulian C, Poloyac SM, Jackson EK, Clark RS, Kochanek PM. The nuclear splicing factor RNA binding motif 5 promotes caspase activation in human neuronal cells, and increases after traumatic brain injury in mice. Journal of cerebral blood flow and metabolism : official journal of the International Society of Cerebral Blood Flow and Metabolism. 2015; 35:655–666.

Jess U, Betz H, Schloss P. The membrane-bound rat serotonin transporter, SERT1, is an oligomeric protein. FEBS letters. 1996; 394:44–46. [PubMed: 8925924]

Jin K, Nagayama T, Mao X, Kawaguchi K, Hickey RW, Greenberg DA, Simon RP, Graham SH. Two caspase-2 transcripts are expressed in rat hippocampus after global cerebral ischemia. Journal of neurochemistry. 2002; 81:25–35. [PubMed: 12067235]

Jin W, Niu Z, Xu D, Li X. RBM5 promotes exon 4 skipping of AID pre-mRNA by competing with the binding of U2AF65 to the polypyrimidine tract. FEBS letters. 2012; 586:3852–3857. [PubMed: 23017209]

Kambeitz JP, Howes OD. The serotonin transporter in depression: Meta-analysis of in vivo and post mortem findings and implications for understanding and treating depression. Journal of affective disorders. 2015; 186:358–366. [PubMed: 26281039]

Kang HJ, Voleti B, Hajszan T, Rajkowska G, Stockmeier CA, Licznerski P, Lepack A, Majik MS, Jeong LS, Banasr M, Son H, Duman RS. Decreased expression of synapse-related genes and loss of synapses in major depressive disorder. Nature medicine. 2012; 18:1413–1417.

Khawaja X, Xu J, Liang JJ, Barrett JE. Proteomic analysis of protein changes developing in rat hippocampus after chronic antidepressant treatment: Implications for depressive disorders and future therapies. J Neurosci Res. 2004; 75:451–460. [PubMed: 14743428]

Kok K, Naylor SL, Buys CHCM. Deletions of the short arm of chromosome 3 in solid tumors and the search for suppressor genes. Adv Cancer Res. 1997; 71:27–92. [PubMed: 9111863]

Laruelle M, Abi-Dargham A, Casanova MF, Toti R, Weinberger DR, Kleinman JE. Selective abnormalities of prefrontal serotonergic receptors in schizophrenia. A postmortem study. Archives of general psychiatry. 1993; 50:810–818. [PubMed: 8215804]

Lee JO, Lee SK, Jung JH, Kim JH, You GY, Kim SJ, Park SH, Uhm KO, Kim HS. Metformin Induces Rab4 Through AMPK and Modulates GLUT4 Translocation in Skeletal Muscle Cells (vol 226, pg 974, 2011). J Cell Physiol. 2012; 227:2804–2804.

Li Y, Roy BD, Wang W, Zhang L, Zhang L, Sampson SB, Yang Y, Lin DT. Identification of two functionally distinct endosomal recycling pathways for dopamine D(2) receptor. The Journal of neuroscience : the official journal of the Society for Neuroscience. 2012; 32:7178–7190. [PubMed: 22623662]

Liao Y, Castello A, Fischer B, Leicht S, Foehr S, Frese CK, Ragan C, Kurscheid S, Pagler E, Yang H, Krijgsveld J, Hentze MW, Preiss T. The Cardiomyocyte RNA-Binding Proteome: Links to Intermediary Metabolism and Heart Disease. Cell Rep. 2016; 16:1456–1469. [PubMed: 27452465]

Loiselle JJ, Roy JG, Sutherland LC. RBM5 reduces small cell lung cancer growth, increases cisplatin sensitivity and regulates key transformation-associated pathways. Heliyon. 2016; 2:e00204. [PubMed: 27957556]

Martinez FJ, Pratt GA, Van Nostrand EL, Batra R, Huelga SC, Kapeli K, Freese P, Chun SJ, Ling K, Gelboin-Burkhart C, Fijany L, Wang HC, Nussbacher JK, Broski SM, Kim HJ, Lardelli R, Sundararaman B, Donohue JP, Javaherian A, Lykke-Andersen J, Finkbeiner S, Bennett CF, Ares M Jr, Burge CB, Taylor JP, Rigo F, Yeo GW. Protein-RNA Networks Regulated by Normal and ALS-Associated Mutant HNRNPA2B1 in the Nervous System. Neuron. 2016; 92:780–795. [PubMed: 27773581]

McCaffrey MW, Bielli A, Cantalupo G, Mora S, Roberti V, Santillo M, Drummond F, Bucci C. Rab4 affects both recycling and degradative endosomal trafficking. FEBS letters. 2001; 495:21–30. [PubMed: 11322941]

Meneses A, Perez-Garcia G, Ponce-Lopez T, Tellez R, Castillo C. Serotonin transporter and memory. Neuropharmacology. 2011; 61:355–363. [PubMed: 21276807]

Mourao A, Bonnal S, Soni K, Warner L, Bordonne R, Valcarcel J, Sattler M. Structural basis for the recognition of spliceosomal SmN/B/B' proteins by the RBM5 OCRE domain in splicing regulation. eLife. 2016; 5

Mourtada-Maarabouni M, Keen J, Clark J, Cooper CS, Williams GT. Candidate tumor suppressor LUCA-15/RBM5/H37 modulates expression of apoptosis and cell cycle genes. Experimental cell research. 2006; 312:1745–1752. [PubMed: 16546166]

Mourtada-Maarabouni M, Sutherland LC, Williams GT. Candidate tumour suppressor LUCA-15 can regulate multiple apoptotic pathways. Apoptosis. 2002; 7:421–432. [PubMed: 12207175]

Nakamura K, Sekine Y, Ouchi Y, Tsujii M, Yoshikawa E, Futatsubashi M, Tsuchiya KJ, Sugihara G, Iwata Y, Suzuki K, Matsuzaki H, Suda S, Sugiyama T, Takei N, Mori N. Brain serotonin and dopamine transporter bindings in adults with high-functioning autism. Archives of general psychiatry. 2010; 67:59–68. [PubMed: 20048223]

O'Bryan MK, Clark BJ, McLaughlin EA, D'Sylva RJ, O'Donnell L, Wilce JA, Sutherland J, O'Connor AE, Whittle B, Goodnow CC, Ormandy CJ, Jamsai D. RBM5 is a male germ cell splicing factor and is required for spermatid differentiation and male fertility. PLoS genetics. 2013; 9:e1003628. [PubMed: 23935508]

Oh JJ, Koegel AK, Phan DT, Razfar A, Slamon DJ. The two single nucleotide polymorphisms in the H37/RBM5 tumour suppressor gene at 3p21.3 correlated with different subtypes of non-small cell lung cancers. Lung Cancer. 2007; 58:7–14. [PubMed: 17606309]

Pagano G, Niccolini F, Fusar-Poli P, Politis M. Serotonin transporter in Parkinson's disease: A meta-analysis of PET studies. Annals of neurology. 2016

Pfeffer S, Aivazian D. Targeting Rab GTPases to distinct membrane compartments. Nature reviews Molecular cell biology. 2004; 5:886–896. [PubMed: 15520808]

Rahbek-Clemmensen T, Bay T, Eriksen J, Gether U, Jorgensen TN. The Serotonin Transporter Undergoes Constitutive Internalization and Is Primarily Sorted to Late Endosomes and Lysosomal Degradation. Journal of Biological Chemistry. 2014; 289:23004–23019. [PubMed: 24973209]

Rajamanickam J, Annamalai B, Rahbek-Clemmensen T, Sundaramurthy S, Gether U, Jayanthi LD, Ramamoorthy S. Akt-mediated regulation of antidepressant-sensitive serotonin transporter function, cell-surface expression and phosphorylation. Biochem J. 2015; 468:177–190. [PubMed: 25761794]

Ray D, Kazan H, Cook KB, Weirauch MT, Najafabadi HS, Li X, Gueroussov S, Albu M, Zheng H, Yang A, Na H, Irimia M, Matzat LH, Dale RK, Smith SA, Yarosh CA, Kelly SM, Nabet B, Mecenas D, Li W, Laishram RS, Qiao M, Lipshitz HD, Piano F, Corbett AH, Carstens RP, Frey BJ, Anderson RA, Lynch KW, Penalva LO, Lei EP, Fraser AG, Blencowe BJ, Morris QD, Hughes TR. A compendium of RNA-binding motifs for decoding gene regulation. Nature. 2013; 499:172–177. [PubMed: 23846655]

Rintala-Maki ND, Sutherland LC. Identification and characterisation of a novel antisense non-coding RNA from the RBM5 gene locus. Gene. 2009; 445:7–16. [PubMed: 19559772]

Sakakibara Y, Kasahara Y, Hall FS, Lesch KP, Murphy DL, Uhl GR, Sora I. Developmental alterations in anxiety and cognitive behavior in serotonin transporter mutant mice. Psychopharmacology. 2014; 231:4119–4133. [PubMed: 24728652]

Sehgal L, Mathur R, Braun FK, Wise JF, Berkova Z, Neelapu S, Kwak LW, Samaniego F. FAS-antisense 1 lncRNA and production of soluble versus membrane Fas in B-cell lymphoma. Leukemia. 2014; 28:2376–2387. [PubMed: 24811343]

Selbach M, Schwanhausser B, Thierfelder N, Fang Z, Khanin R, Rajewsky N. Widespread changes in protein synthesis induced by microRNAs. Nature. 2008; 455:58–63. [PubMed: 18668040]

Stenmark H. Rab GTPases as coordinators of vesicle traffic. Nat Rev Mol Cell Bio. 2009; 10:513–525. [PubMed: 19603039]

Storvik M, Haukijarvi T, Tupala E, Tiihonen J. Correlation between the SERT binding densities in hypothalamus and amygdala in Cloninger type 1 and 2 alcoholics. Alcohol Alcoholism. 2008; 43:25–30. [PubMed: 18039673]

Thomas AJ, Hendriksen M, Piggott M, Ferrier IN, Perry E, Ince P, O'Brien JT. A study of the serotonin transporter in the prefrontal cortex in late-life depression and Alzheimer's disease with and without depression. Neuropathology and applied neurobiology. 2006; 32:296–303. [PubMed: 16640648]

van der Lee R, Lang B, Kruse K, Gsponer J, Sanchez de Groot N, Huynen MA, Matouschek A, Fuxreiter M, Babu MM. Intrinsically disordered segments affect protein half-life in the cell and during evolution. Cell Rep. 2014; 8:1832–1844. [PubMed: 25220455]

van der Sluijs P, Hull M, Webster P, Male P, Goud B, Mellman I. The small GTP-binding protein rab4 controls an early sorting event on the endocytic pathway. Cell. 1992; 70:729–740. [PubMed: 1516131]

Wu X, Lan L, Wilson DM, Marquez RT, Tsao WC, Gao P, Roy A, Turner BA, McDonald P, Tunge JA, Rogers SA, Dixon DA, Aube J, Xu L. Identification and validation of novel small molecule disruptors of HuR-mRNA interaction. ACS chemical biology. 2015; 10:1476–1484. [PubMed: 25750985]

Yuen EY, Liu W, Karatsoreos IN, Ren Y, Feng J, McEwen BS, Yan Z. Mechanisms for acute stress-induced enhancement of glutamatergic transmission and working memory. Molecular psychiatry. 2011; 16:156–170. [PubMed: 20458323]

Zhang J, Cui Z, Feng G, Bao G, Xu G, Sun Y, Wang L, Chen J, Jin H, Liu J, Yang L, Li W. RBM5 and p53 expression after rat spinal cord injury: implications for neuronal apoptosis. The international journal of biochemistry & cell biology. 2015; 60:43–52. [PubMed: 25578565]

Zhu CB, Lindler KM, Campbell NG, Sutcliffe JS, Hewlett WA, Blakely RD. Colocalization and Regulated Physical Association of Presynaptic Serotonin Transporters with A(3) Adenosine Receptors. Mol Pharmacol. 2011; 80:458–465. [PubMed: 21705486]

HIGHLIGHTS

- Rab4 Levels are increased in RBM5 Knockdown Neurons vs. Controls.
- Oligomeric SERT Levels are decreased in RBM5 Knockdown Neurons vs. Controls.
- Monomeric SERT Uptake/Endocytosis is increased in RBM5 Knockdown Neurons vs. Controls.
- RBM5 is a Novel Regulator of Rab4 Signaling in Neurons.

A

Culture Isolation #	SAMPLE #	Group ID	Estimated [RNA]	260/230	260/280
Neuron Density 5X10^6/10cm2 Dish					
1	Sample 1	NT-siRNA-GFP	930.30µg/mL	2.403	2.141
1	Sample 2	Rbm5-siRNA-GFP	294.75µg/mL	2.356	2.739
1	Sample 3	DDK-E Control	368.98µg/mL	2.019	2.186
1	Sample 4	RBMF-ORF	715.69µg/mL	2.254	2.098
2	Sample 6	DDK-E Control	455.39µg/mL	2.35	2.392
2	Sample 7	RBMF-ORF	519.31µg/mL	2.23	2.16
3	Sample 8	NT-siRNA-GFP	1052.1µg/mL	2.245	2.153
3	Sample 9	Rbm5-siRNA-GFP	1038.6µg/mL	2.188	2.12
3	Sample 10	DDK-E Control	1227.7µg/mL	2.22	2.097
3	Sample 11	RBMF-ORF	793.45µg/mL	2.306	2.372
4	Sample 12	NT-siRNA-GFP	843.33µg/mL	2.249	2.077
4	Sample 13	Rbm5-siRNA-GFP	794.81µg/mL	2.243	2.047
4	Sample 14	DDK-E Control	720.45µg/mL	2.34	2.151
4	Sample 15	RBMF-ORF	664.82µg/mL	2.431	2.148

B

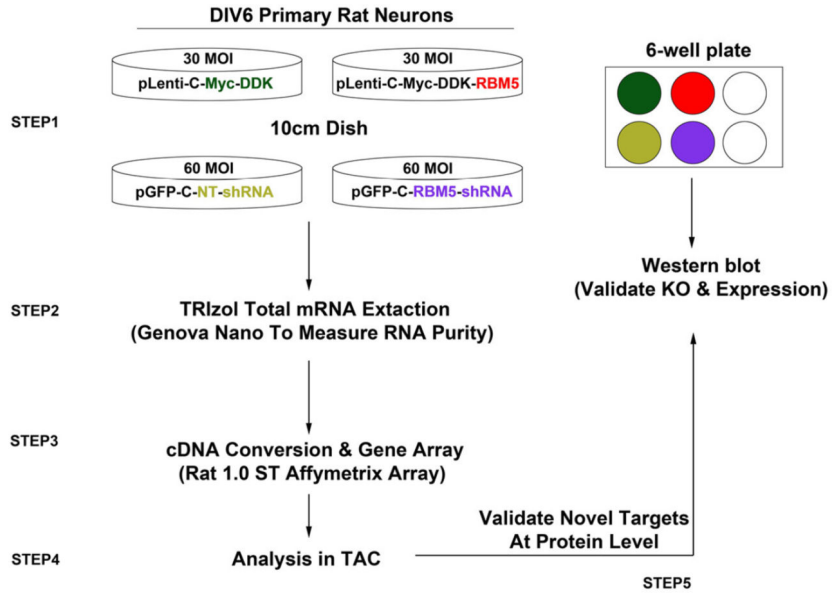

Figure 1. Illustration of Experimental Study Design & Validation of High-Quality RNA Samples Used in Microarray Analysis

(A) RNA purity was analyzed on a Genova Nano. In all samples 260/230 and 260/280 ratios were > 2.0 (indicating ultra-pure RNA). **(B)** Illustration of experimental design. Three to four independent culture isolations (i1, i2, i3, and i4) were done in which four different viral vectors were used; control overexpression vector (green), recombinant rat RBM5 overexpression (red), non-targeting shRNA control vector (yellow), and RBM5 targeting shRNA (purple). Four 10cm dishes and one 6-well culture plate were prepared for each individual culture isolation experiment. Neurons in 10cm dishes were harvested for total RNA. Neurons in 6 well-plates were harvested for protein.

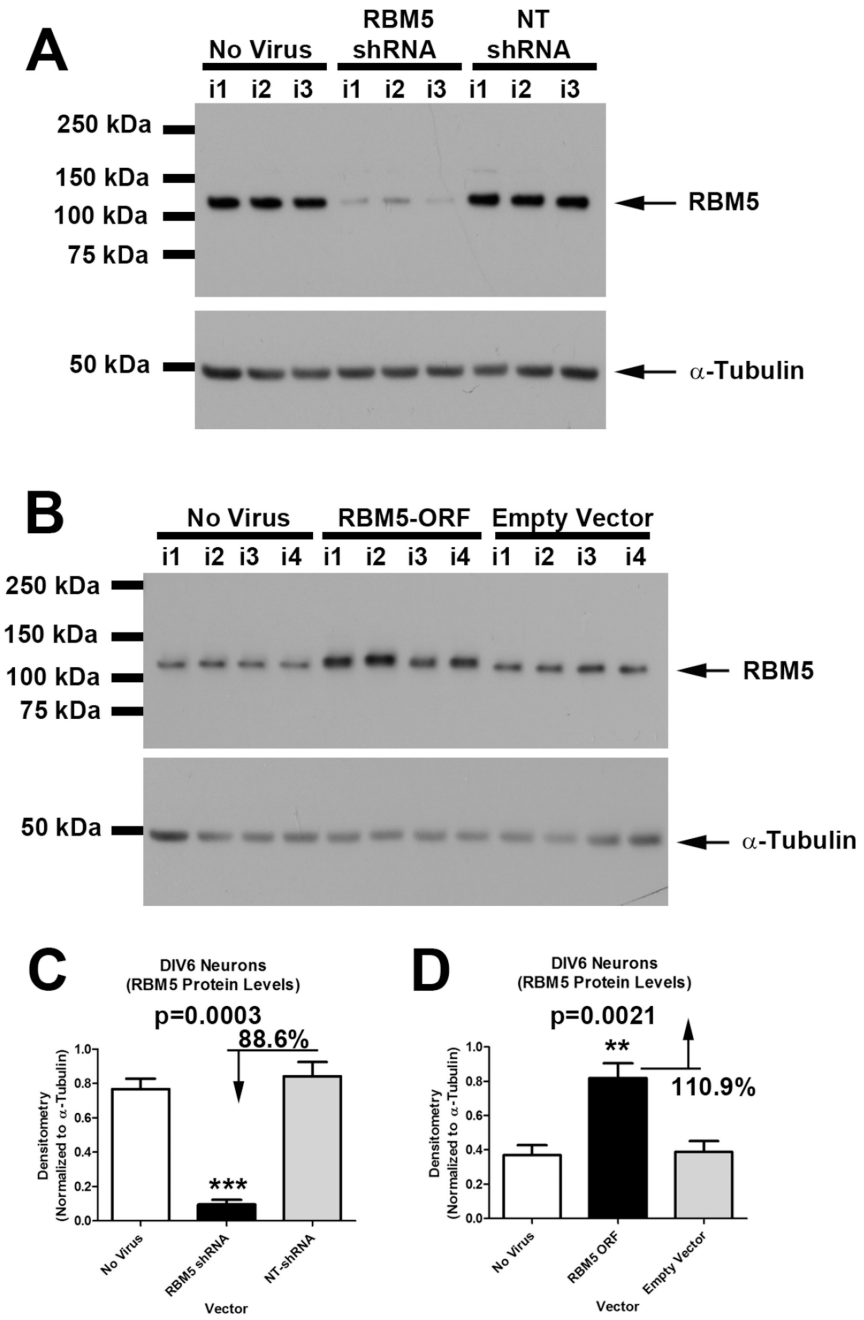

Figure 2. Validation of RBM5 Protein KO vs. Overexpression in Neuron Culture Experiments Also Used for Microarray Analysis

(A) Western blot shows neurons which were not given virus, transduced with RBM5 targeting shRNA or transduced with non-targeting (NT) shRNA control. **(C)** Densitometry confirms a ~88.6% decrease in RBM5 levels in KO samples. **(B)** Western blot shows neurons which were not given virus, transduced with an RBM5 overexpression vector, or transduced with an empty vector control. **(D)** Densitometry confirms a ~2 fold increase in RBM5 levels vs. empty vector control. Multiple comparisons were analyzed by one-way-

ANOVA and Newman-Keuls post-hoc test. Data were significant at $p < .05$ (*). Graphs show mean + SEM.

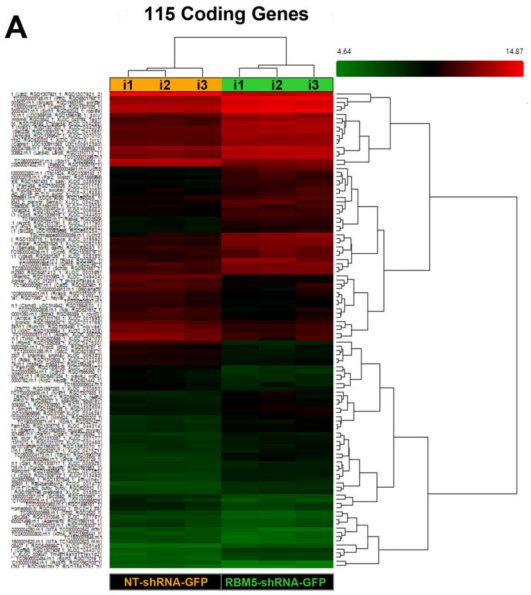

B **Top 10 Gene Hits (NT vs. RBM5 KO)**

GENE ID	NT-GFP Signal	KO Signal	Fold Change	ANOVA p-value	FDR p-value	Description (Involved in)
Sec23a	11.53	13.02	2.79	0.000003	**0.069**819	ER to Golgi Transport
RBM5	10.82	8.33	-5.63	0.000002	**0.069**819	Splicing Factor (**Study Target**)
Rab4a	9.11	10.71	3.03	0.000002	**0.069**819	Small GTPase/Endocytosis
Capns1	11.06	12.17	2.16	0.000041	0.092777	Calpain 1 subunit/Proteolysis
Pfn2	10.47	12.16	3.23	0.000023	0.092777	Profilin-2-like/Actin binding
Pfn2	12.55	14.59	4.13	0.000024	0.092777	Profilin-2/Cytoskeletal Regulator
Syt11	13.24	14.49	2.38	0.000049	0.092777	Ca^{2+} Binding and transport
Tprg1l	7.68	9.35	3.17	0.000027	0.092777	Found in Synaptic Vesicles
Sox11	13.4	12.34	-2.08	0.000058	0.092777	Cell Proliferation
Cpne8	6.18	7.67	2.81	0.000056	0.092777	Extracellular Vesicular Exosomes

C **Real-Time PCR (Comparative C_T)**

Gene	Average C_T (Three Independent Exp.)	ΔC_T (Target Gene-GAPDH)	$\Delta\Delta C_T$ (ΔC_T Target – ΔC_T Calibrator)	$2^{-\Delta\Delta CT}$ (Fold Diff. Relative to NT-Control Levels)
Rab4a	25.86 ± 0.15	5.6 ± 0.16	-1.25 ± 0.16	2.4 (2.1-2.7)
Sec23a	25.68 ± 0.16	5.42 ± 0.17	-0.85 ± 0.17	1.8 (1.6-2.0)

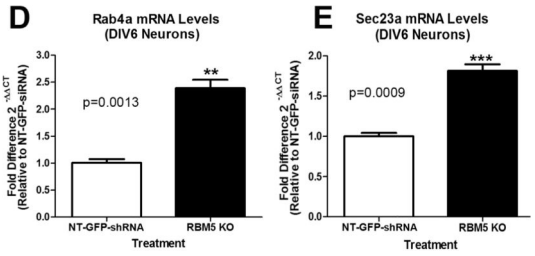

Figure 3. Identification of Novel RBM5 Regulated Gene Targets in Primary Cortical Neurons

Neurons were transduced with lentivirus to overexpress NT-shRNA or RBM5 targeting shRNA (n=3 independent experiments). Total RNA were harvested at DIV6, and samples analyzed by rat specific microarrays to probe expression levels of 24,753 coding mRNAs. **(A)** Dendrogram shows 115 coding mRNAs that were differentially expressed in control vs. RBM5 KO neurons (before FDR correction). Samples labeled i1, i2, i3 are from different cortical isolation experiments/viral transductions done on different days. Heat map shows genes with relative increased expression (Red) or decreased expression (Green). **(B)** The top 10 genes with the greatest fold change in expression comparing NT controls vs. RBM5 KO

neurons. **(C–E)** Quantitative Real-Time PCR analysis of Sec23a and Rab4a mRNA in control vs. RBM5 KO neurons (n=3 independent experiments). Data were analyzed by unpaired T-test. Data were significant at $p < .05$ (*). Graphs show mean + SEM.

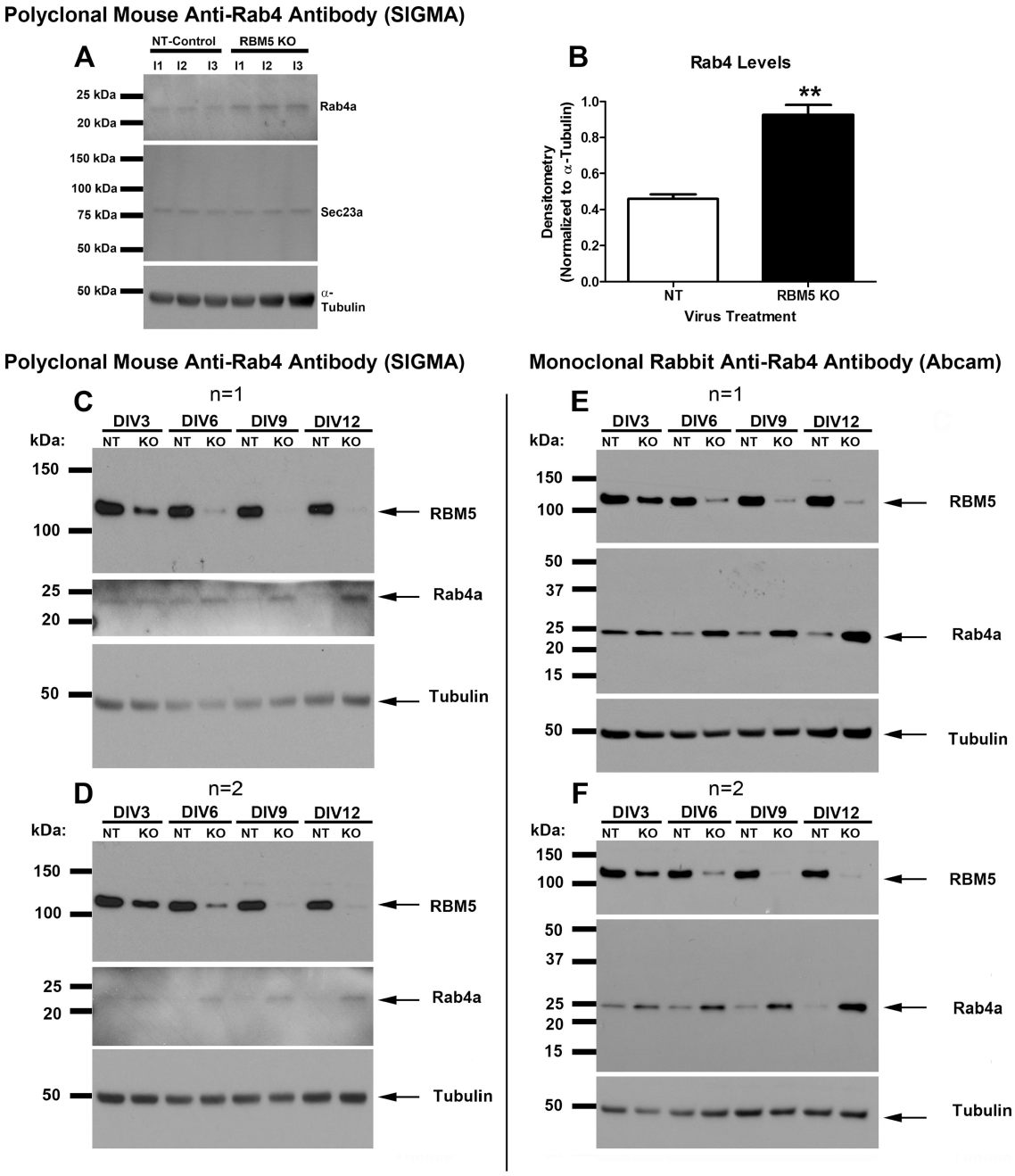

Figure 4. Rab4a Protein is increased in KO vs. Control Samples as Measured by Two Different Antibodies

(A) Western blots show that Rab4a protein (but not Sec23a) is increased in KO neurons relative to controls in three independent neuron culture isolation experiments (i1, i2, i3), as detected by a mouse polyclonal antibody (SIGMA). **(B)** Densitometry shows significant increase in Rab4a levels in KO neurons vs. controls. (**C–F**) Neurons were transduced with lentivirus to overexpress NT-shRNA or RBM5 targeting shRNA and protein extracts were harvested between DIV3-DIV12. Two biological replicates (n=1 and n=2) were prepared/ harvested from a single neuron culture isolation experiment. (**C** and **D**) Age course samples

were probed with anti-RBM5, anti-Rab4 (SIGMA, Mouse Polyclonal), and anti-α-Tubulin antibodies. (**E** and **F**) Age course samples were probed with anti-RBM5, anti-Rab4 (Abcam, Rabbit Monoclonal), and anti-α-Tubulin antibodies. Data were analyzed by unpaired T-test. Data were significant at $p < .05$ (*). Graphs show mean + SEM.

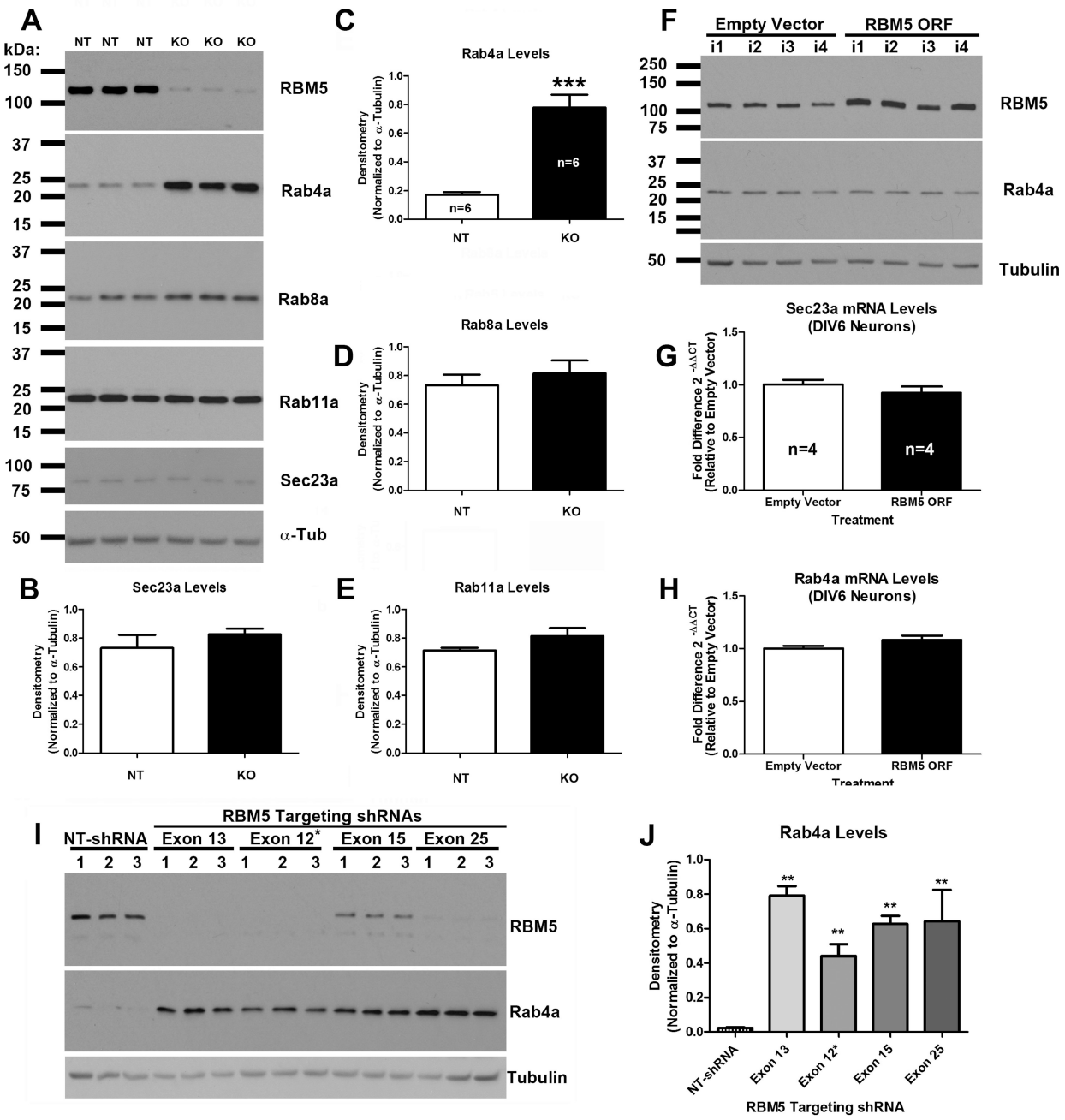

Figure 5. Only Rab4a Levels are altered in KO Neurons vs. Controls

Neurons were transduced with lentivirus to overexpress NT-shRNA or RBM5 targeting shRNA. Protein extracts were harvested DIV12. **(A)** Representative Western blots (n=3/group) show changes in RBM5, Rab4a, Rab8a, Rab11a, Sec23a and α-Tubulin in RBM5 KO neurons vs. NT controls. **(B–E)** Densitometry of Sec23a, Rab4a, Rab8a, and Rab11a in DIV12 cortical neurons (n=6/group). **(F)** RBM5 overexpression does not affect Rab4 protein levels in DIV6 cortical neurons (four independent samples corresponding to culture isolations in microarray studies). (**G** and **H**) RBM5 overexpression does not affect Sec23a or Rab4a mRNA levels in DIV6 cortical neurons, respectively. **(I)** The exon 12* targeting

RBM5 shRNA was used in microarray screening studies as well as in SERT endocytosis studies. Three alternative RBM5 targeting shRNAs also increase Rab4a levels vs. NT controls in DIV12 cortical neurons. (**J**) Densitometry of Rab4a changes by different RBM5 targeting shRNAs. In Panels **B–E** and **G–H** data were analyzed by unpaired T-test. Data were significant at $p < .05$ (*). In Panel **J** data were analyzed by 1-Way-ANOVA followed by Newman-Keuls post-hoc test. (**) = $p < .001$, (***) = $p < .0001$. Graphs show mean + SEM.

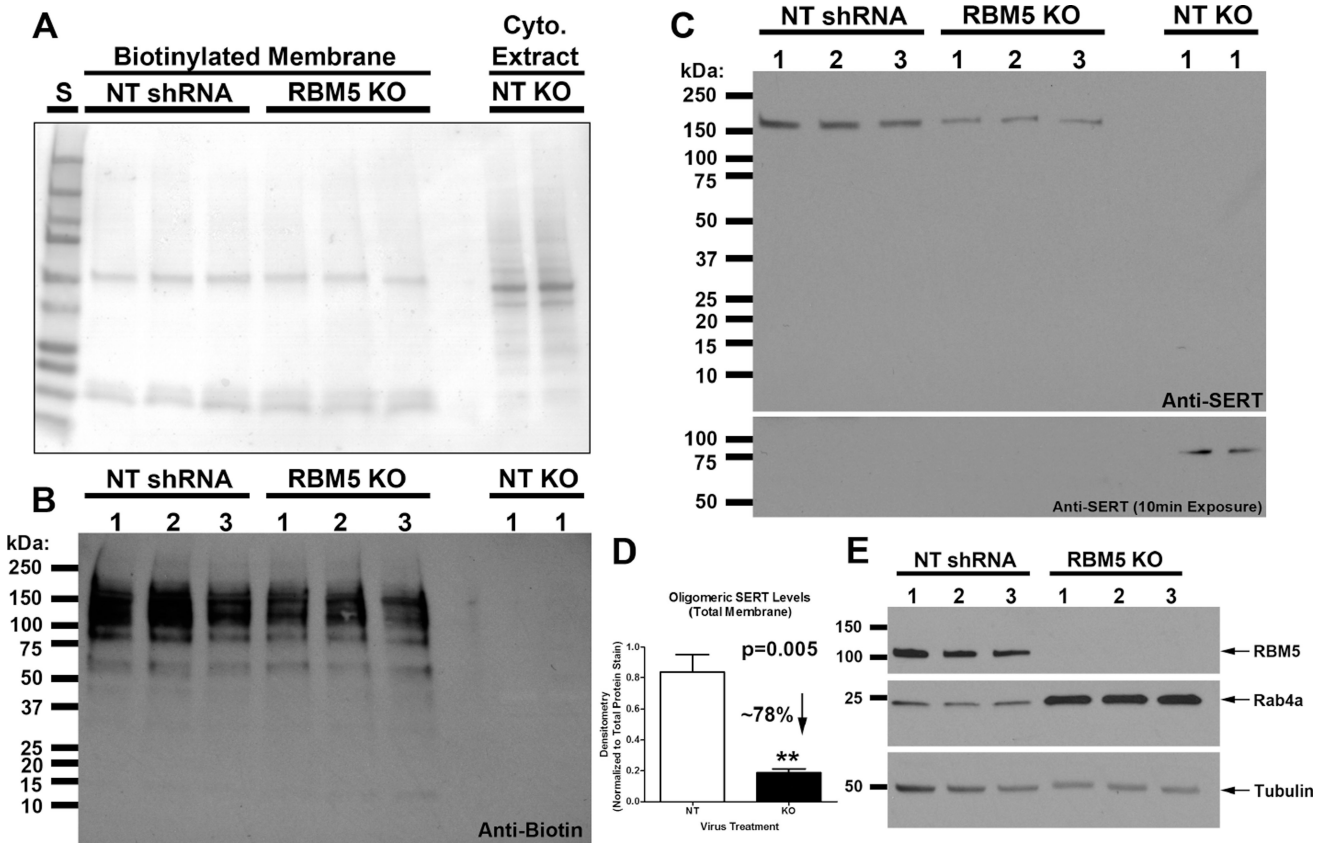

Figure 6. Oligomeric SERT Membrane Levels are decreased in RBM5 KO vs. Control Neurons

Neurons were transduced with lentivirus to overexpress NT-shRNA or RBM5 targeting shRNA. DIV12 neuronal membrane proteins were conjugated with irreversible biotin linker and harvested for protein analysis. **(A)** Total membrane stain shows marked difference in biotinylation derived extracts vs. cytoplasmic fraction, and also shows equal loading comparing NT vs. KO biotinylation extracts. **(B)** Anti-biotin antibody shows that biotinylated proteins are not detected in cytoplasmic extracts. **(C)** Anti-SERT antibody shows a marked decrease in oligomeric SERT membrane levels in KO extracts vs. NT control. A longer exposure time (lower image) shows monomeric SERT is present in cytoplasmic fractions but levels do not differ by condition. **(D)** Densitometry shows that oligomeric SERT is decreased by ~78% in KO neurons vs. controls. **(E)** Confirmation that RBM5 is decreased, and Rab4a is increased, in cytoplasmic fractions of KO vs. NT samples used for biotinylation/membrane SERT analysis. Data were analyzed by unpaired T-test. Data were significant at $p < .05$ (*). Graphs show mean + SEM.

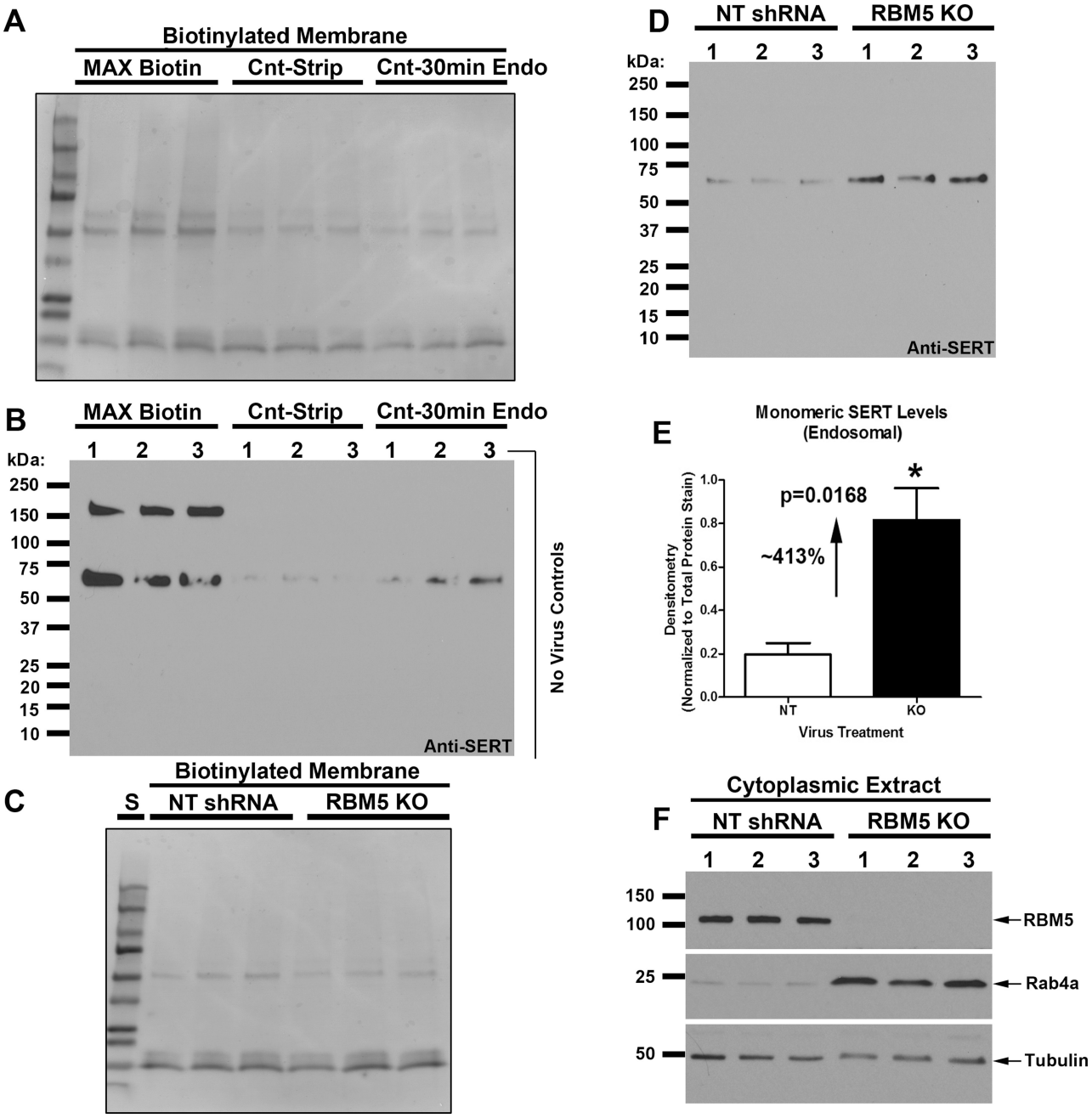

Figure 7. Intracellular Uptake of Monomeric Membrane-Derived SERT is increased in RBM5 KO vs. Control Neurons

The endocytosis assay to detect SERT was validated using non-transduced DIV12 control neurons conjugated with a reversible biotin linker, given a brief 30min endocytosis period, and harvested for protein analysis. **(A)** Total membrane stain shows loss of signal in samples subject to glutathione stripping (to remove membrane biotin) vs. MAX-Biotin samples (which did not receive a glutathione strip). **(B)** Anti-SERT antibody shows that (a) oligomeric and monomeric SERT is detected in MAX-Biotin control neurons, (b) neither SERT form is detected in control neurons given a glutathione strip but not given a 30min endocytosis period (Cnt-Strip), and (c) only monomeric SERT is detected in neurons given a

30min endocytosis period and which was subsequently followed by a glutathione strip (Cnt-30min-Endo). **(C)** Neurons were transduced with lentivirus to overexpress NT-shRNA or RBM5 targeting shRNA, and prepared for analysis of 30min SERT endocytosis at DIV12 using our validated assay. Total membrane stain shows relative equal gel loading in biotinylated derived NT vs. KO extracts. **(D)** Anti-SERT antibody shows a marked increase in monomeric SERT endocytosis in KO extracts vs. NT controls. **(E)** Densitometry shows that monomeric SERT is increased by ~413% in KO neurons vs. controls. **(F)** Confirmation that RBM5 is decreased, and Rab4a is increased, in cytoplasmic fractions of KO vs. NT samples used for biotinylation/endocytosed SERT analysis. Data were analyzed by unpaired T-test. Data were significant at $p < .05$ (*). Graphs show mean + SEM.

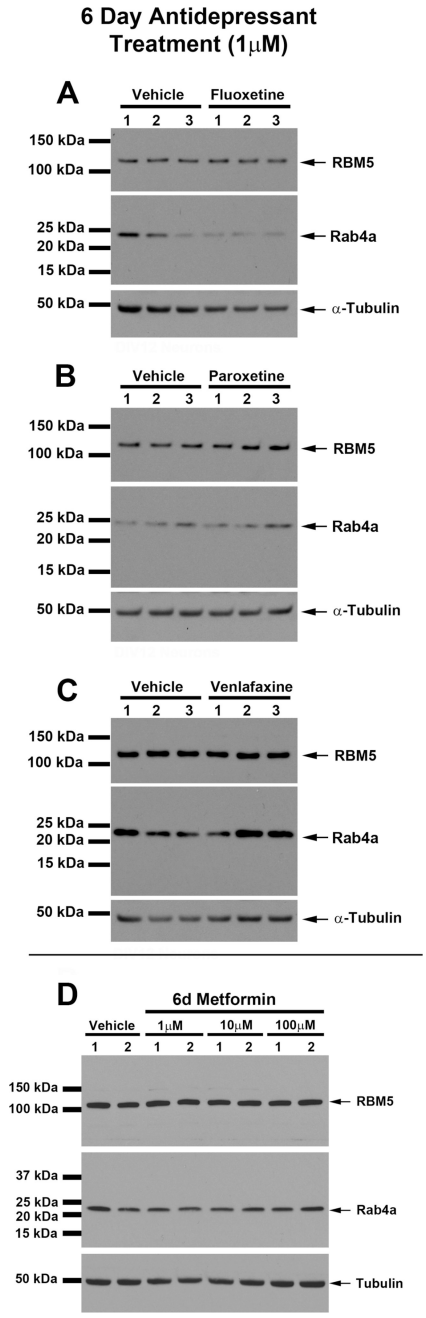

Figure 8. Effect of Chronic SSRIs or Metformin Treatment on Rab4a/RBM5 Protein Levels in Neurons

DIV6 cortical neurons were treated with 1μM **(A)** fluoxetine, **(B)** paroxetine, or **(C)** venlafaxine for a total of 6d and subsequently harvested at DIV12. Antidepressants did not increase Rab4a. RBM5 levels were unaffected by SSRIs. **(D)** Similarly, 6d treatment with 1–100μM metformin did not increase Rab4a levels or alter RBM5 in DIV12 neurons.